Review

Structural Studies on the Bacteriophage Φ6 and Its Transformations during Its Life Cycle

J Bernard Heymann *

Posted Date: 25 October 2023

doi: 10.20944/preprints202310.1587.v1

Keywords: Cystoviridae; cryoEM; dsRNA; ssRNA; RNA-dependent RNA polymerase; virus capsid; virus envelope; virus infection

Review

Structural Studies on the Bacteriophage Φ6 and Its Transformations during Its Life Cycle

J Bernard Heymann [1,2,*]

[1] National Institute of Arthritis and Musculoskeletal and Skin Diseases, National Institutes of Health, 50 South Dr, Bethesda, MD 20892, USA; heymannb@mail.nih.gov
[2] National Cryo-EM Program, Cancer Research Technology Program, Frederick National Laboratory for Cancer Research, Leidos Biomedical Research, Inc., Frederick, MD 21701, USA; heymannb@mail.nih.gov
* Correspondence: heymannb@mail.nih.gov; Tel.: 301-846-6924

Abstract: From the first isolation of the cystovirus bacteriophage Φ6 from *Pseudomonas syringae* 50 years ago, we have progressed to a better understanding of the structure and transformations of the many parts of the virion. The three-layered virion encapsulating the tripartite double stranded RNA (dsRNA) genome, breaches the cell envelope on infection, generates its own transcripts, and coopts the bacterial machinery to produce its proteins. The generation of new virions starts with a procapsid with a contracted shape, followed by packaging single stranded RNA segments with concurrent expansion of the capsid, and finally replication to reconstitute the dsRNA genome. The outer two layers are then added, and the fully formed virions released by cell lysis. Most of the procapsid structure composed of the proteins P1, P2, P4 and P7 is now known, as well as its transformations to the mature, packaged nucleocapsid. The outer two layers are less well studied. One additional study investigated the binding of the host protein YajQ to the infecting nucleocapsid, where it enhances the transcription of the large RNA segment that codes for the capsid proteins. Finally, we relate the structural aspects of bacteriophage Φ6 top those of other dsRNA viruses, noting the similarities and differences.

Keywords: Cystoviridae; cryoEM; dsRNA; ssRNA; RNA-dependent RNA polymerase; virus capsid; virus envelope; virus infection

1. The Significance of Bacteriophage Φ6

The members of the Cystoviridae are the only known double-stranded RNA (dsRNA) bacteriophages, with bacteriophage Φ6 the first isolated and type species of the family [1]. They represent counterparts to the dsRNA infecting eucaryotes and offer simpler systems for studies of structure and life cycle. These involve questions such as how the genome is encapsidated in the protective virus shells [2], and the roles of the component proteins in the propagation of the virus. Such insights may lead to the development of antivirals and treatments for managing pathogenic viruses [3]. In addition, the presence of dsRNA is typically a sign of viral infection [4].

The host of bacteriophage Φ6, *Pseudomonas syringae* (previously known as *P. phaseolicola*) is a plant pathogen of commercial importance in agriculture. One potential use for such a phage is therefore in controlling bacterial infections in plants [5,6].

In recent years, bacteriophage Φ6 has been used as a surrogate for enveloped viruses such as SARS-Cov-2 [3]. Used with care to acknowledge the differences [7], it can be a valuable tool to understand environmental factors associated with viral infectivity without undue exposure to a dangerous virus.

 doi:10.20944/preprints202310.1587.v1

2. The Life Cycle of Bacteriophage Φ6

The Φ6 virion is composed of multiple layers, with the P1 protein forming an icosahedral capsid shell enclosing the dsRNA genome, in turn surrounded by an intermediate shell composed of proteins P4 and P8, and finally covered by an outer protein-lipid shell or envelope (Figure 1). The genome itself is divided into three parts, the small (S), medium (M) and large (L) segments of dsRNA.[1] The segments code for proteins at the different stages of the life cycle [9]. On infection, virions first bind to the host pili [1], requiring the protein P3 anchored onto P6 [10]. The pili then retracts and the virions fuse with the outer membrane mediated by the P6 protein [10]. The lysin (protein P5) then degrades the peptidoglycan layer [11,12], allowing viral particle transport across the inner membrane in an energy-dependent manner [13]. The P8 layer is then stripped off and degraded [13]. What remains is the nucleocapsid[2], decorated with the P4 protein on the outside and producing ssRNA transcripts. Unique to Φ6, a host protein, YajQ, binds to the outside of the nucleocapsid to enhance the transcription of the L segment [14]. The transcripts from all three segments are exported and translated to the different viral proteins by the host machinery.

The four translation products of the l segment, P1, P2, P4 and P7, assemble into procapsids [15,16]. The three ssRNA segments are then sequentially packaged into the capsid [17], with concurrent expansion. The minus strand synthesis (replication) follows the completion of the packaging of the l segment [8]. The P8 layer is then assembled onto the new nucleocapsids [13]. The non-structural protein, P12, is required by P9 to form the proteolipid envelope, with incorporation of proteins P3, P6, P10 and P13 [18]. The proteins P5 and P10 cause cell lysis and the release of the virions [11,19].

The quantitation of the copy number of every protein is important in understanding the assembly and transformations of the virion and its sub-particles during the life cycle [20]. In the following section I will cover not only the structure, but also the copy numbers of the various proteins and how that relates to function. There will also be references to the structures of the related viruses, such as Φ8 and Φ12. These show some sequence similarity, but with very similar genomic organization protein structures [21].

---

[1] The segments are denoted in lower case for single stranded RNA and in upper case for double stranded RNA. See 8. Frilander, M.; Poranen, M.; Bamford, D.H. The large genome segment of dsRNA bacteriophage phi6 is the key regulator in the in vitro minus and plus strand synthesis. *RNA* **1995**, *1*, 510-518. for examples.

[2] The term nucleocapsid is used with or without the P8 layer.

Preprints (www.preprints.org) | NOT PEER-REVIEWED | Posted: 25 October 2023 doi:10.20944/preprints202310.1587.v1

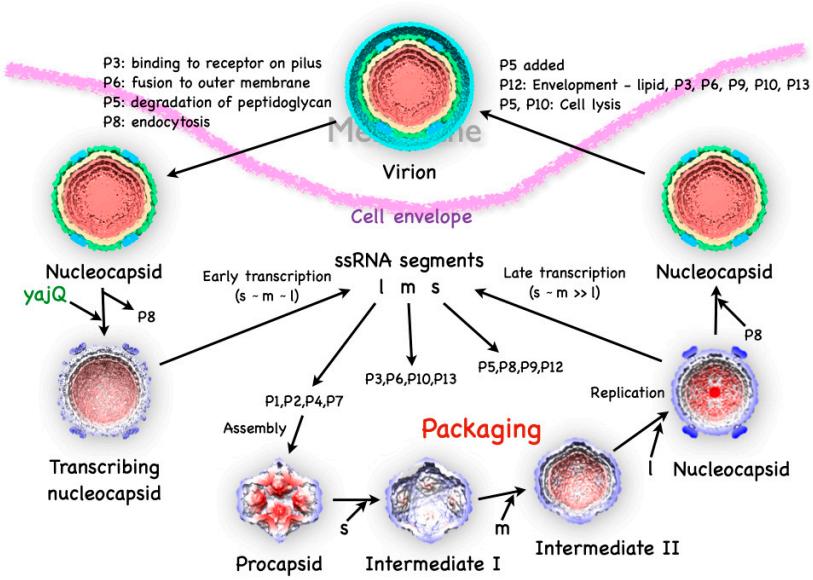

Figure 1. The bacteriophage Φ6 life cycle in structures. The virion has three layers surrounding the tripartite dsRNA genome (red): the capsid (beige), the intermediate layer (blue & green) and the proteolipid envelope (cyan). Infection starts with the P3 protein in the envelope binding to the pilus receptor, followed by outer membrane fusion (P6), degradation of the peptidoglycan layer (P5) and entry mediated by P8. After P8 disassembles, the host factor YajQ binds to facilitate the transcription of the l segment, so that it is expressed at about the same levels as the s and m segments. The l segment codes for the four proteins assembled into the initial product, the procapsid. The ssRNA segments are then packaged in sequence with corresponding expansion of the capsid shell. Once all the segments are packaged, replication completes the production of the dsRNA genome. The P8 shell is assembled, the envelope added, and the virion released through cell lysis.

3. The Initial Assembly Product, the Procapsid

The procapsid (also called the polymerase complex) consists of four proteins [15]: P1 that makes up the icosahedral shell, P2, the RNA-dependent RNA polymerase (RdRP) [22], P4, the packaging motor [23,24], and P7, an assembly and packaging enhancer [25,26]. Early attempts to crystallize the procapsid failed, opening the way for studies by electron microscopy. As will be discussed later, the procapsid is in a metastable state, and the P4 protein is a hexamer in a symmetry-mismatch position with fragile association with the P1 shell. These factors may not be conducive to stable crystal contacts and required imaging by electron microscopy of fresh samples soon after preparation.

3.1. The P1 Shell

The main part of the procapsid consists of an icosahedral shell formed by the 85 kDa P1 protein [27]. Early cryoEM reconstructions revealed a compact particle with invaginated file-fold vertices, giving it a star-like appearance (Figure 2A) [28–33].

The stoichiometry of the virion indicated that there are 120 copies of the P1 protein per particle [20], which means there are two copies per asymmetric unit, similar to other dsRNA viruses (Figure 2C) [28,34]. Better cryoEM reconstructions allowed the discernment of structural details of the two copies [29] and eventually to near-atomic detail [35]. The architecture is very similar in the related bacteriophage Φ8 [36].

While the whole procapsid could not be crystallized, a pentamer of P1 in the presence of P7 was solved (Figure 2B) [35]. Similarly, a pentamer of the P1 from Φ8 was also solved by X-ray crystallography (El Omari, 2013 #9598}. The pentamer forms the invaginated five-fold vertices and the subunits are designated as $P1_A$ (blue in Figure 2C). The other subunits are designated as $P1_B$, connecting the two-fold and three-fold axes (red/orange/yellow in Figure 2C). $P1_A$ and $P1_B$ have

Preprints (www.preprints.org) | NOT PEER-REVIEWED | Posted: 25 October 2023 doi:10.20944/preprints202310.1587.v1

identical folds with only minor differences in conformation to adapt to their different positions in the capsid[3] [35].

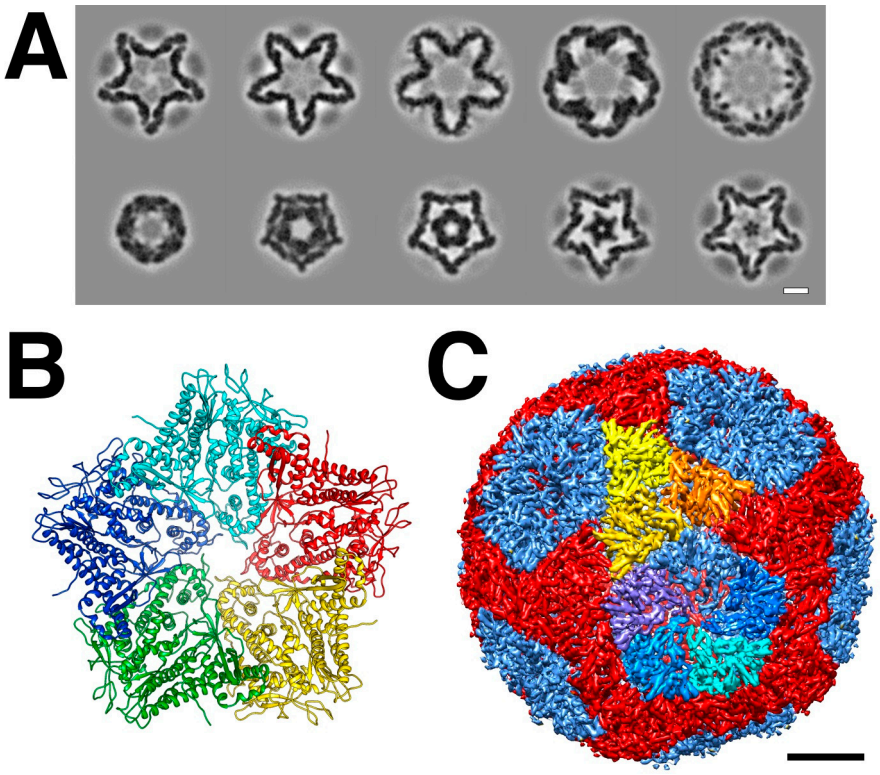

Figure 2. The procapsid shell. (A) Sections through a procapsid showing the invaginated five-fold vertices of the P1 shell. The diffuse densities are the minor procapsid proteins. (EMDB: 1501) [30] (B) The pentamer of P1 solved by X-ray crystallography. (PDB: 4K7H) [35] (C) Distinction of the $P1_A$ (blues) and $P1_B$ (red, orange, yellow) subunits in the procapsid. Scale bars: 100 Å.

3.2. The Packaging Motor, Protein P4

The 35 kDa protein P4 was identified as an NTPase required for the packaging of positive ssRNA strands into the procapsid [23,24]. The P4 protein forms a hexamer [38,39] that sits in the five-fold invagination in the procapsid with an obvious symmetry mismatch [40]. Both in virions, as well as recombinant and assembled procapsids, about 60-70 P4 monomers per particle was reported, close to the expected 72 (12 hexamers) [41]. In bacteriophage Φ8 nucleocapsids, the average occupancy of P4 on the five-fold vertices were found to be ~60 [42]. However, isolated Φ6 procapsids in other studies were consistently at lower copy numbers (Table 1). Increased ionic strength, heat and acidic conditions lead to P4 dissociation and procapsid expansion [31,43,44]. The interaction between P4 and P1 is therefore rather weak, perhaps tuned to intracellular conditions differing significantly from those in isolates.

Both available high resolution procapsid reconstructions have very low P4 density [35,45], precluding assessing its association with the P1 shell. It is likely that the same interaction is maintained in the nucleocapsid, where we have several reconstructions. An asymmetric reconstruction of the five-fold vertex shows the P4 hexamer on top of the P1 shell and surrounded by the P8 layer (Figure 3A,C) [46]. Because of the symmetry mismatch, only some of the protrusions from the hexamer is expected to interact with P1. In Figure 3B the thresholding of the isosurface was adjusted to show four possible connections. Sun et al. [46] identified a density not attributed to the P1 shell but consistent with the C-terminal tail of P4 (Figure 3D). The C-terminal 13 residues were

[3] An example of "quasi-equivalence" of the subunits of the capsid 37. Caspar, D.L.; Klug, A. Physical principles in the construction of regular viruses. *Cold Spring Harb Symp Quant Biol* **1962**, *27*, 1-24..

Preprints (www.preprints.org) | NOT PEER-REVIEWED | Posted: 25 October 2023 doi:10.20944/preprints202310.1587.v1

previously shown to be important for procapsid assembly [47]. This tail extends over both the P1A and P1B subunits. The density is strong enough to suggest that five of the six P4 C-termini bind to the P4 shell. In procapsids, P4 is often shifted slightly from the five-fold axis [31], suggesting some of its C-terminal tethers may be less tightly bound.

Table 1. Stoichiometry of procapsids assembled in vivo from proteins expressed from cDNA.

Composition	Method*	P2	P4	P7	Reference
P1247	C	8	5#	-	[31]
	D	7	25	10	[33]
	S	4	29	12	[33]
	D	10		34	[32]
P124	D	6	31		[33]
	S	4	40		[33]
	D	6			[32]
P147	D		33	3	[33]
	S		35	12	[33]
	D			11	[32]
Maximum		20	72	60	

* C: Counts in tomograms; D: Map density; S: SDS-PAGE. # Most P4 released by increased salt concentration in preparation.

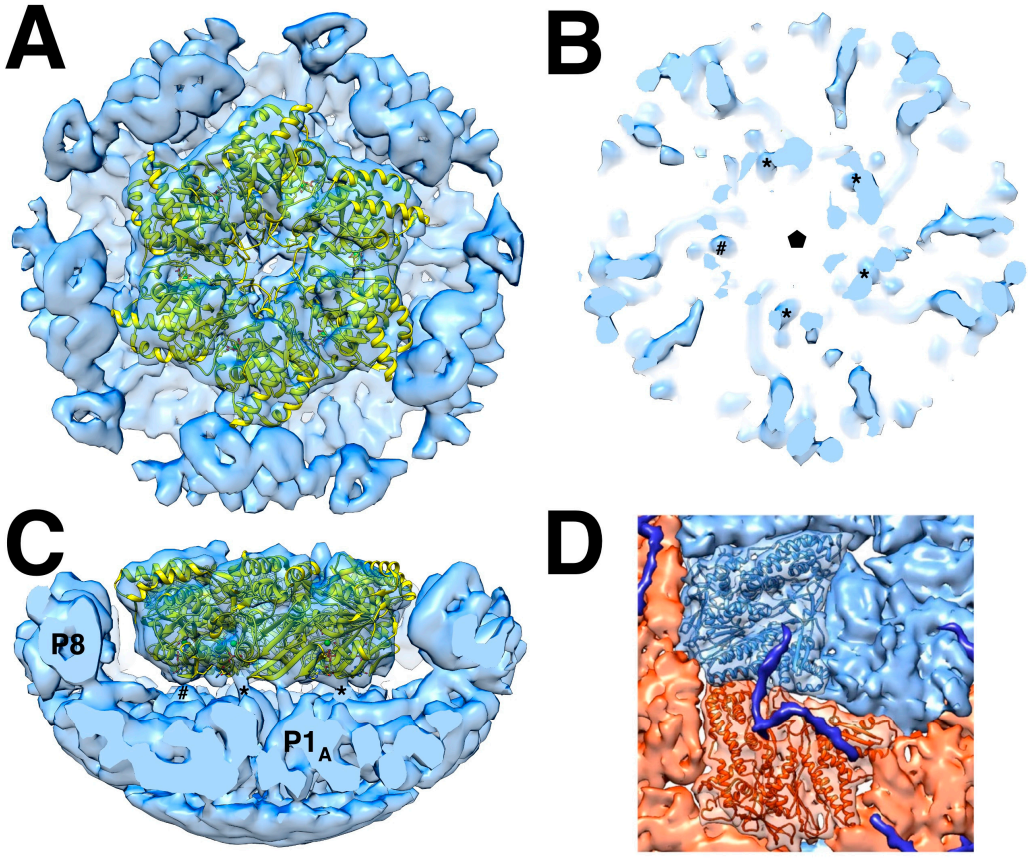

Figure 3. The packaging motor, P4: (A) The P4 X-ray crystal structure (PDB: 5MUV) fitted into the density of an asymmetric reconstruction of the five-fold vertex of the nucleocapsid (EMDB: 3573), surrounded by the P8 layer. (B) A section through the reconstruction at the contact plane reveals four possible connections (stars), with the fifth (ampersand) not quite forming a connection. (C) Side view showing the connections between P4 and capsid shell below. (D) The C-terminal tail of P4 (blue) traverses the surfaces of P1A (light blue) and P1B (red) [46].

Preprints (www.preprints.org) | NOT PEER-REVIEWED | Posted: 25 October 2023 doi:10.20944/preprints202310.1587.v1

3.3. The RNA-Dependent RNA Polymerase, Protein P2

The whole Φ6 procapsid was functionally referred to as the polymerase complex because of its activity in transcription and replication [48,49]. The 75 kDa protein P2 was identified as the actual polymerase responsible for both replication and transcription [22], and its structure was solved by X-ray crystallography [50].

The polymerase is self-priming with emphasis on the first two nucleotides at the 3' of the ssRNA template fitting into a pocket of the C-terminal domain [50,51]. It can replicate a variety of ssRNA and stimulated by manganese [22]. Manganese appears to lessen the specificity of the polymerase for the 3' terminal sequence [52] by decreasing stability [53], suggesting a mechanism for regulation of its activity. Manganese consistently enhances activity for related polymerases from Φ6, Φ 8 and Φ 13, but with different magnitudes [54], reflecting subtle variations in structure. The self-priming is dependent on the presence of the C-terminal domain linked through residues 601-614 [51]. Manganese destabilizes the interface of the C-terminal domain to allow for permissive elongation [55]. A mutant in the manganese binding site (E491Q) stabilizes the C-terminal domain, desensitizing it to the stimulatory effect of manganese [53]. This becomes more important in the context of the infection cycle, where Φ6 developed a mechanism for controlling the production of the l transcript by exploiting the host protein, YajQ (see section 6) [56].

In the early cryoEM reconstructions of the procapsid, P1 and P4 were readily assigned to densities [40], but the locations of both P2 and P7 were not evident. The P2 protein was only located when it was noticed that there is a persistent density on the 3-fold axis inside the procapsid (Figure 4A-C) [30]. Because it exists as a monomer, there is a symmetry mismatch and its density in the cryoEM map is reduced, explaining why it was originally missed. An asymmetric cryoEM reconstruction of the location of P2 on the three-fold axis yielded a map that provided the proper orientation of the molecule (Figure 4D,E) [45]. Specific interactions with P1 in the palm and fingers domains were confirmed by mutational analysis [57].

Knowing where P2 is located, it can be identified in cryo-electron tomograms of individual procapsids, allowing quantitation by counting (Table 1, first row) [31]. The average occupancy was found to be about 8 out of the 20 possible sites with a distribution that indicates random incorporation during procapsid assembly. This agrees with dose-dependent incorporation during in vitro assembly of procapsids [41,57].

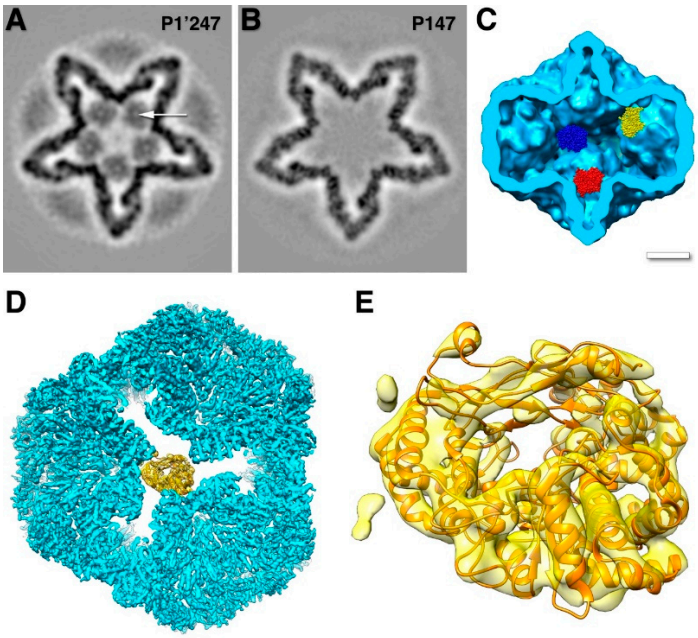

Figure 4. The location of the polymerase in the procapsid. (A) Section through a reconstruction of the procapsid showing the location of the polymerase (arrow). (EMDB: 1501) (B) Section through a reconstruction of a procapsid lacking the polymerase. (EMDB: 1502) (C) Isosurface rendering of a cut

Preprints (www.preprints.org) | NOT PEER-REVIEWED | Posted: 25 October 2023 doi:10.20944/preprints202310.1587.v1

through the P1 shell of the procapsid with three polymerase atomic models arranged in the locations indicated in A [30]. Scale bar: 100 Å. (D) The polymerase (yellow) within the P1 shell (blue) viewed down a three-fold axis. (EMDB: 3185) (E) Fit of the polymerase crystal structure within the reconstructed density within the context of the P1 shell (EMDB: 3186; PDB: 5FJ6) [45].

3.4. The Packaging Enhancer, Protein P7

The 17 kDa protein P7 enhances assembly of the procapsid and packaging, but is not essential in either function [25,26,41,58]. The location of P7 in the procapsid was shrouded in mystery for a time. The only known structure is the N-terminal part of the homologous protein in bacteriophage Φ12 (Figure 5B) [59]. Because it was solved as a dimer, the prevailing assumption was that it would be a dimer in the procapsid. It was reported as such a dimer within the intermediate layer, outside the P1 shell [60]. Neutron scattering could only provide a rough radius for both P2 and P7, with P7 possibly located either inside or outside the capsid [61]. Earlier reconstructions of procapsids with and without P7 did not produce any meaningful results [30,40]. With better data and higher resolution maps, P7 was eventually located inside P147 procapsids on the sides of the invaginated five-fold vertices (Figure 5A) [32,33].

These sites overlap with the location of P2, indicating that the substoichiometric amounts are the result of competitive binding [33]. In assembled procapsids with a large excess of P7, ~60 copies of P7 incorporated into each particle and the inclusion of P2 is suppressed [41]. However, at about a stoichiometric ratio, the copy number was only ~45 for P7 and 11 for P2 [41], closer to the numbers for recombinant procapsids (Table 1). From these findings the expected maximum copy numbers are ~30 for P7 and ~10 for P2, with any excess attributed to non-binding inclusion in in vitro assembled particles. Both these proteins appear to be functional in substoichiometric amounts.

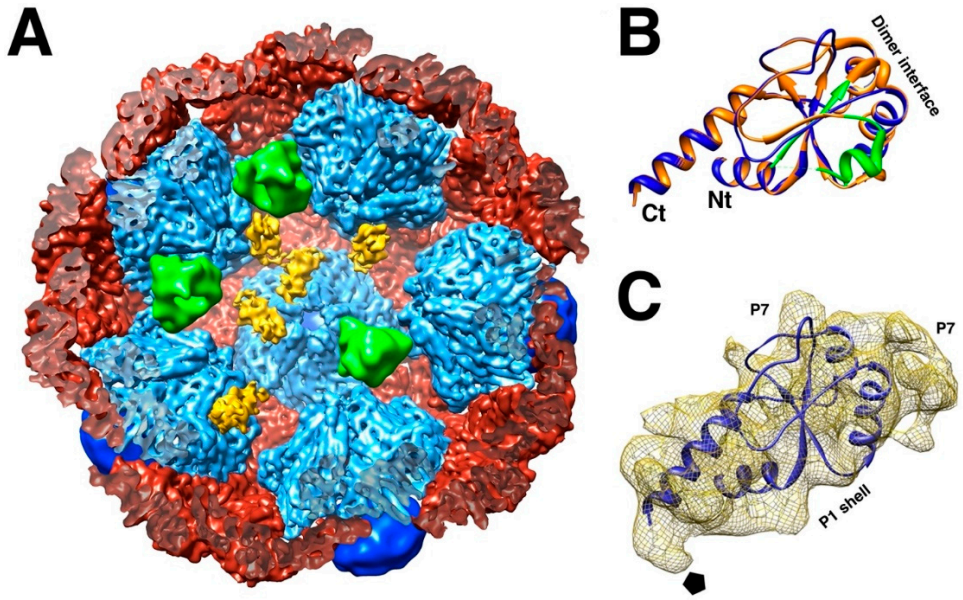

Figure 5. The location of P7. (A) Each P7 monomer (yellow) is bound to the interface between two P1A subunits (light blue), but only at some locations around the five-fold axis. Polymerase monomers (green) are located at other sites that overlap with the P7 sites. The P1B subunits (red) and P4 hexamers (dark blue) completes the procapsid. (EMDB: 2341) (B) Homology model of the f6 P7 based on the crystal structure of the f12 P7 protein N-terminal fragment. The dimer interface in the crystal is indicated. (C) One P7 density with a fit of the homology model. Also indicated are the interface to the P1 shell, and the interfaces to two potential P7 neighbors around the three-fold axis. The pentagon denotes the five-fold axis. [33].

Preprints (www.preprints.org) | NOT PEER-REVIEWED | Posted: 25 October 2023 doi:10.20944/preprints202310.1587.v1

3.5. Procapsid Assembly

As is common for many other virus capsids, the procapsids of Φ6 readily assembles from recombinant constructs in vivo or purified proteins in vitro. The simplest procapsid that can be assembled is P14 from proteins P1 and P4, while P1 alone or with P7 forms unstable particles in cells but are fragile to isolation [16]. P1 can assemble into a pentamer in the presence of P7, although P7 was not detected in crystals [35]. In bacteriophage Φ8, P1 assembled into a pentamer by itself [62]. A minimal first product is likely a pentamer of $P1_A$ with P4. The C-terminal tail of P4 extends beyond the $P1_A$ to $P1_B$ [46], suggesting that it could stabilize the addition of $P1_B$ subunits to the pentamer.

Both P2 and P7 accelerates assembly [57,58]. P2 incorporates in a dose-dependent manner [57], consistent with the random placement at the 20 binding sites [31]. If P2 and P7 are not in the mixture before assembly, they are excluded if added afterward, consistent with their internal location [41]. P2 sits in between three invaginated five-fold vertices (Figure 4D) [45], while P7 covers an interface between $P1_A$ subunits (Figure 5A) [33]. The presence of all three accessory proteins therefore aids in the efficient production of the P1 shell and acts as the scaffolding commonly observed in other viruses [63].

The sequence of assembly events is uncertain beyond the initial pentamer, likely with a P4 hexamer and 2-3 copies of P7. The potential next step is the addition of $P1_B$ subunits with the involvement of the P4 C-terminal tail. Conceptually, the $P1_{10}P4P7_{2-3}$ units could then come together to form the icosahedral shell with P2 binding between some neighboring $P1_A$ pentamers.

4. Packaging of the ssRNA Segments and Capsid Expansion

The packaging of plus strand RNA in the cystoviruses differ from their eucaryotic counterparts [2]. Cystoviruses package in typical bacteriophage style by insertion into a preformed procapsid driven by a motor protein. Instead, in the Reoviridae, the ssRNA first assembles into a particle serving as the nucleating core for the assembly of the capsid shell [64].

From the early cryoEM work on Φ6, it was clear that the procapsid expands to assume its mature form in the nucleocapsid [28]. The internal volume increases by ~2.5 fold to accommodate the full dsRNA genome [29,43]. Concurrent with expansion, the genomic ssRNA segments package in a strict order, with the s segment first, followed by m and l [17]. The specificity is dependent on conditions, with higher magnesium (> 4 mM) and phosphate (> 1.5 mM) concentrations rendering the packaging non-specific. Once the l segment is packaged, the polymerase replicates the segments to produce the dsRNA genome [8].

The sequential order of packaging indicates that there should be two expansion intermediates, but only one was identified in the original structural study [28]. A second expansion intermediate was found where nucleocapsids lost their dsRNA [43]. The first intermediate is readily obtained by mild heat, acid or ionic strength conditions [43,44], indicating that the first expansion energy barrier is relatively low. The presence of 10x excess of P2 in assembled procapsids appears to prevent expansion [57]. This suggests that the binding of P2 between the invaginated five-fold vertices is strong enough to stabilize the procapsid. On expansion to first intermediate, P2 is not apparently associated with the P1 shell any more [43]. The ease with which the first intermediate is obtained means that it is the more stable conformation of the P1 shell (Figure 6). Presumably, the packaging of the s segment is enough to trigger the first expansion event. The low efficiency of packaging [65] impeded efforts to observe the entry of the s segment by cryoEM.

The current understanding is that the procapsid exists in a metastable state that is easily triggered to expand to intermediate 1, either by acid, heat or salt, and potentially by the packaging of the s segment generating some pressure inside the procapsid (Figure 6) [43]. The packaging of the m and l segments then increases the pressure on the P1 shell, with it reaching the fully mature state and pressurized state after replication. In reconstructions of the nucleocapsid, the regions around the 5-fold vertices are still flexible, indicating that they don't reach the level of stability of the rest of the capsid.

The demonstration that only one P4 hexamer per procapsid is necessary for packaging following by minus strand synthesis (replication) led to the proposal that there is a special vertex different from

Preprints (www.preprints.org) | NOT PEER-REVIEWED | Posted: 25 October 2023 doi:10.20944/preprints202310.1587.v1

the others [66]. One possible consequence of such special vertex is that one would expect there to be a correlation between the locations of P4 hexamer on the outside and the polymerase on the inside. No such correlation was found in a tomographic study of procapsids where individual proteins were counted [31]. It was concluded that such a special vertex is unlikely.

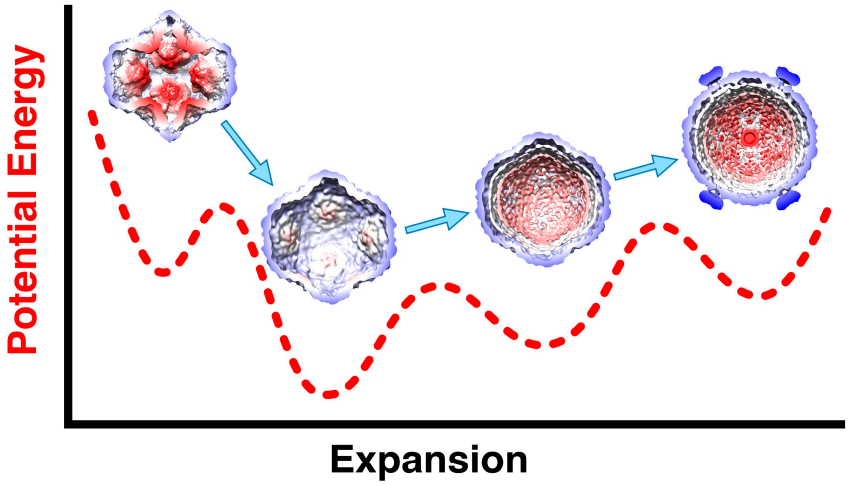

Figure 6. The transformations of the P1 shell on maturation with the dashed curve showing a conceptional energy profile along the expansion coordinate. The procapsid readily converts to the first expansion intermediate by various triggering events such as heat, acid or salt, or the packaging of the s segment. Packaging the m segment then leads to further slight expansion to the second intermediate, followed by packaging the l segment. Only then is the genome replicated to produce the full dsRNA complement.

5. Completing the Virion

5.1. The dsRNA Packaging of the Nucleocapsid

Remarkably, the dsRNA genome packages in a few configurations amenable to reconstruction such that the helical strands are clear (Figure 7A,B) [67]. In the cypoviruses, defined conformations of the dsRNA have also been found [68,69]. This means that the icosahedral capsids of the dsRNA viruses form very specific interactions with the genome. This is despite the current understanding that the packaging mechanisms are different. While the cystoviruses package their three ssRNA segments into preformed procapsids, the eucaryotic dsRNA viruses form their capsids around preassembled particles containing the 9-12 ssRNA segments within organized cellular structures called viral factories or viroplasms [2]. How these particles come together is complex and still requires intensive study [70].

While the dsRNA in Φ6 is arranged in ordered shells (Figure 7B), P2 and P7 are apparently not in detectable locations [33,45]. This contrasts with the cypoviruses where 10 transcriptional enzyme complexes, each composed of a polymerase and a packaging NTPase, locate to specific sites [68,69]. Somehow, during Φ6 transcription, P2 should be positioned at a five-fold vertex to allow a newly synthesized transcript to be ejected by P4. In Φ12, a density that could be P2 was shown underneath the five-fold vertices in virions [60]. Since there are only three segments, conceptually requiring three polymerases, they may not be distributed in regular locations conducive to the extensive averaging in cryoEM reconstruction.

Preprints (www.preprints.org) | NOT PEER-REVIEWED | Posted: 25 October 2023 doi:10.20944/preprints202310.1587.v1

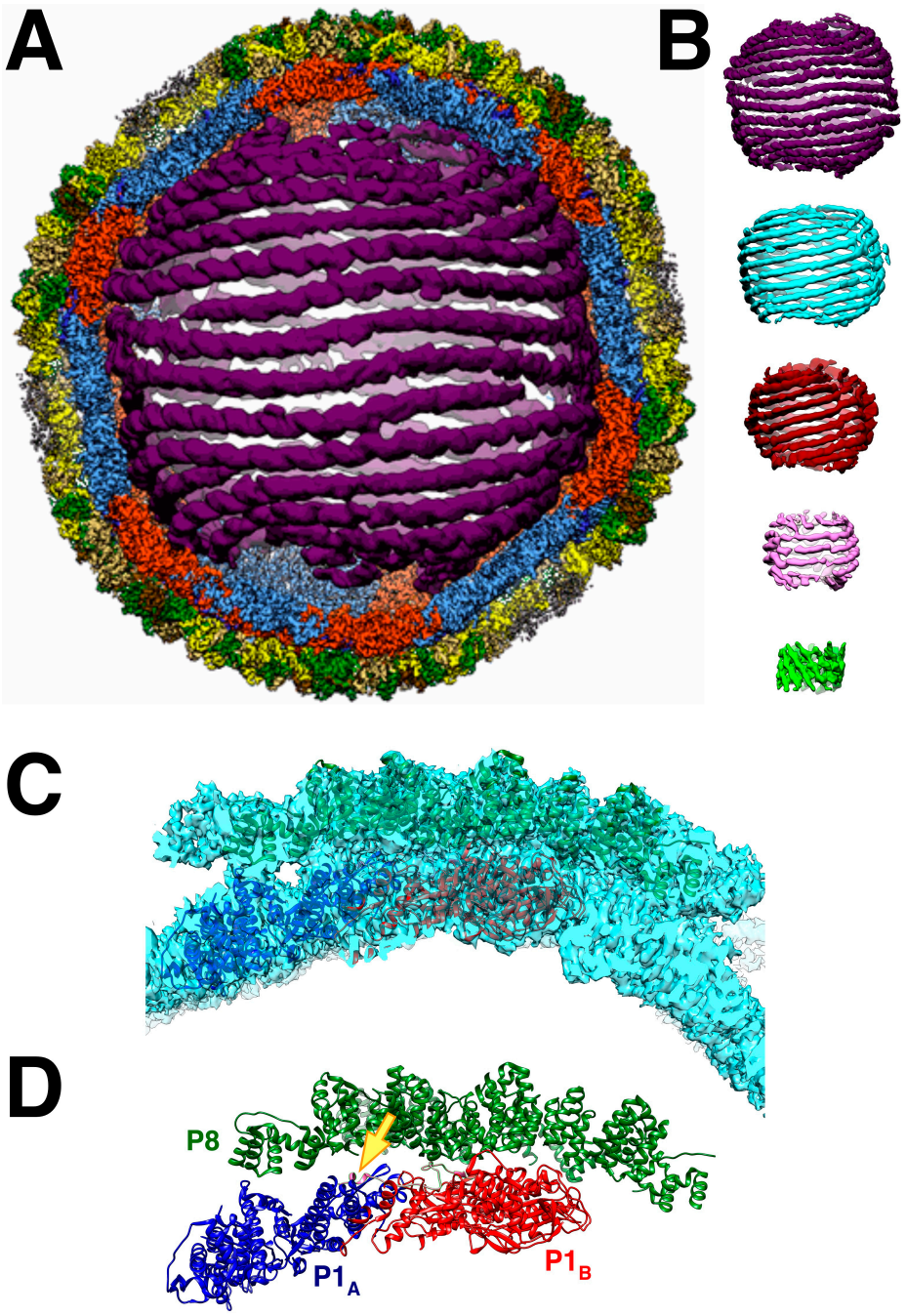

Figure 7. (A) The nucleocapsid orientated down a two-fold axis, showing a cut through the outer two layers and the first shell of dsRNA. The outer shell is the P4-P8 layer, but in this cut view, only the P8 layer is visible (green). The capsid shell is composed of the P1A (blue) and P1B (red) proteins. (B) The five dsRNA shells. (C) Two P1 subunits and 10 P8 monomers fitted into a reconstruction of the nucleocapsid. (D) As in C but without the density. The arrow points to the P4 C-terminal tail (pink) bound to the two P1 subunits [67].

5.2. The Intermediate Layer Composed of P4 and P8

The P8 layer is composed of 200 trimers arranged in a T = 13*laevo* quasi-symmetric lattice with openings at the five-fold vertices to accommodate the P4 hexamers [46]. The interactions between the trimers show complicated domain-swapping features.

The P4 occupancy in the nucleocapsid is close to stoichiometric [41,67], indicating that it is assembled as such in the procapsid. The observation of lower amounts on purified procapsids (Table 1) should therefore be considered an artifact of purification. The Φ8 P4 hexamer is offset by 8 Å from

 doi:10.20944/preprints202310.1587.v1

the five-fold axis of the P1 shell [42], likely the result of the symmetry mismatch with only up to five of the six C-terminal tails binding it to the P1 shell [46].

The assembly of the 16 kDa P8 protein onto the nucleocapsid requires calcium, and it can be stripped off by removing calcium [13]. Purified P8 can also self-assemble into spherical shells in the presence of calcium, but mostly without closing [13,71]. The location where calcium binds is not known. The assembled nucleocapsid with P8 is infective in cells where the outer membrane and peptidoglycan layers have been disrupted [13]. P8 binds to host phospholipids [72]. During infection, P8 interacts with the cell membrane to form invaginations around the nucleocapsid, with P8 degraded in the cytoplasm to release the P8 devoid nucleocapsid [73]. The nucleocapsid coated with P8 has significantly lower polymerase activity as compared to the procapsid [13], such that its uncoating and degradation promotes polymerase activity.

5.3. The Envelope

The envelope of Φ6 is the least studied structurally because it does not conform to the icosahedral symmetry of the inner two layers. It is composed of host lipids [74] and the proteins P3, P5, P6, P9 and P10 [75,76] and requires P12 for proper formation [18]. P5, the lysozyme of Φ6, is thought to be located between the envelope and the P4-P8 shell [77]. P9 is the major integral membrane protein, accompanied by P6 and P10 [77,78]. In E. coli, P9 expression leads to the formation of P9-containing vesicles, with P12 playing a protective role in preventing the proteolytic degradation of P9 [79]. The most prominent feature of the envelope are the mushroom-like spikes protruding from the surface, identified as P3 and anchored to the membrane by P6 [80]. The equivalent multichain P3 of Φ12 is a hexameric spike [81].

6. Coopting the Host Factor YajQ for Transcription Regulation

After breaching the bacterial envelope of its host and losing the P8 layer, the Φ6 nucleocapsid transcribes its genome to produce the three ssRNA segments [82]. It was noticed that nucleocapsids produced *in vitro* also show suppressed expression of the L segment, unless manganese was included [83–85]. The l segment differs from the s and m segments in the second nucleotide: it is 5'-GU rather than 5'-GG. This renders the nucleocapsid unable to transcribe the l segment, or any segment starting with anything other than 5'-GG [8,56]. Manganese at 1 mM overrules this blockage by increasing the permissivity of the polymerase [8,52,53]. Mn competes with Mg at the non-catalytic metal ion binding site in the polymerase [55]. However, the concentrations of manganese in the host do not reach the levels required for activating the polymerase, indicating a different mechanism.

Qiao et al. [14] discovered that the nucleocapsid binds an 18 kDa host protein, YajQ, required for full transcription of the L segment. YajQ homologues are ubiquitous and conserved in bacteria [86]. However, YajQ is specific for Φ6 transcription, while another cystovirus, Φ2954, requires GrxC [87]. A YajQ-GFP fusion protein coats infecting Φ6 capsids to such an extent that the individual particles were visible inside cells [88]. Later in infection when many new nucleocapsids are produced, the supply of YajQ is insufficient, yielding fewer l transcripts. This is interpreted as a fortuitous regulatory function to divert resources to the other segments during final virion assembly. YajQ binds to the outside surface of the nucleocapsids, and dissociates in higher salt concentration [14]. Because YajQ does not activate the polymerase directly [56], it must act through the capsid shell with the polymerase on the inside.

Purified nucleocapsids decorated with YajQ (Figure 8A) was visualized by cryoEM (Figure 8B) [89]. The micrographs show many filled capsids, but also empty P1 shells likely derived from packaged capsids that lost their RNA content (Figure 8B) [43]. YajQ binds as a monomer to 60 sites close to the three-fold axes of the icosahedral P1 shell, in this case with an occupancy of ~58 % (35 out of 60 sites) (Figure 8C). A homology model of YajQ based on the crystal structure from *Haemophilus influenzae* [90] fits unambiguously into the 3D reconstruction, indicating conservation of the fold (Figure 8D). The YajQ structure features two topologically similar domains connected by two linkers. Each domain has a beta sheet on one side and two alpha helices on the other. Each YajQ molecule

Preprints (www.preprints.org) | NOT PEER-REVIEWED | Posted: 25 October 2023 doi:10.20944/preprints202310.1587.v1

straddles the two P1 subunits in the asymmetric unit, covering part of the C-terminal tail of P4 (purple density in Figure 8D).

Purified polymerase still shows the discrimination against the l segment [22], but YajQ has no effect on it [56]. The evidence points to the stability of the C-terminal domain and its role in the self-priming initiation of transcription. Manganese relieves the requirement of the Φ6 nucleocapsids for YajQ, decreasing template specificity [56]. Mutations in two of the genes confer YajQ independence: I632V in P1, and K34N and I642V in P2 [14]. Other mutations in the hinge region of the C-terminal domain (V603A, A604E and L612R) increases activity in nucleocapsids in the absence of YajQ, presumably by destabilizing this domain [56].

An additional density was noted close to where YajQ binds (Figure 8D) [89] that turns out to be the C-terminal tail of P4 first described by Sun et al. [46]. This may suggest a way of action. YajQ may stabilize the tail of P4 to such an extent that it affects the expression of the l segment. If so, the slight change at the 5' end of the l transcript may pose a higher barrier for transcription.

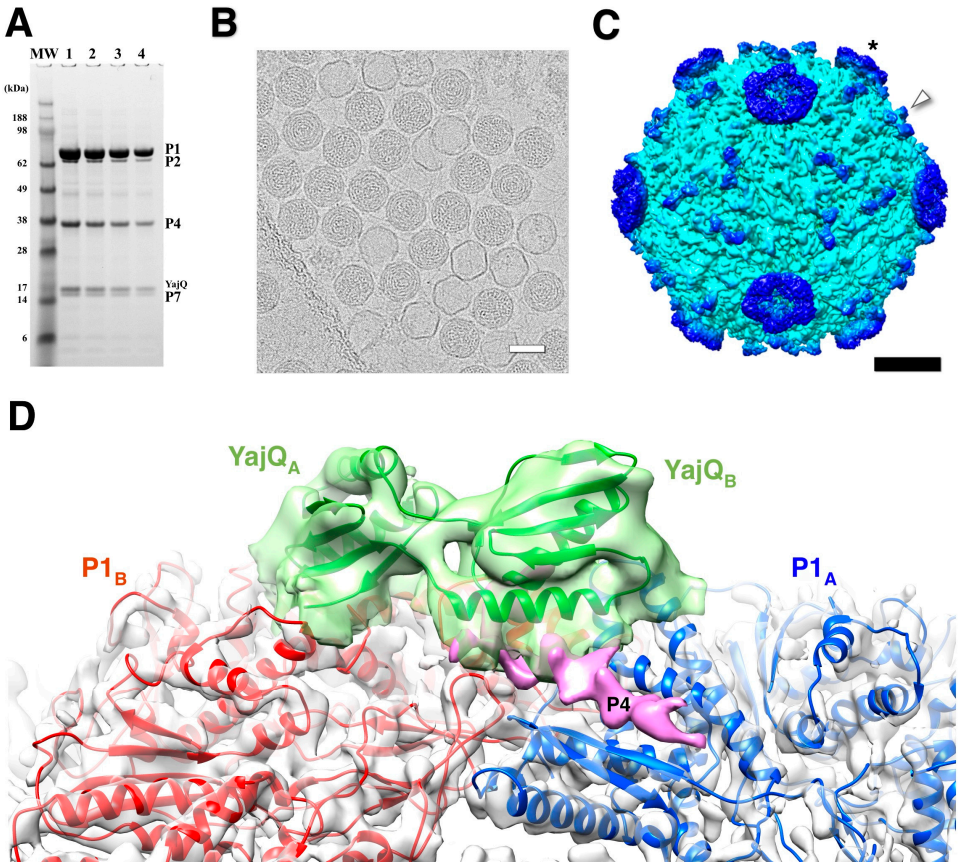

Figure 8. The bacteriophage φ6 nucleocapsid with bound YajQ. (A) SDS-PAGE gel showing the four constituent proteins together with YajQ at a slightly larger amount than P7. (B) A representative micrograph of YajQ-bound packaged capsids with a few empty P1 shells. Scale bar: 500 Å. (C) A reconstruction of the nucleocapsid filtered to 6 Å. The YajQ monomers (arrowhead) are bound to sites surrounding the three-fold vertices. The P4 hexamers (asterisk) are the donut densities suspended above the five-fold vertices. Scale bar: 100 Å. (D) Fit of a homology model of YajQ (green) into the density attached to the capsid. Also shown are the two capsid subunits, $P1_A$ (blue) and $P1_B$ (red), and a purple density consistent with the C-terminal tail of P4 [89].

7. The Broader Impact of the Studies on the Structure and Transformations of Bacteriophage Φ6

We have made significant progress in understanding the Φ6 life cycle, but much remains to be discovered. This relatively simple system provided some answers about dsRNA viruses and structural studies benefitted from recent technological advances as well as contributed to the development of new experimental approaches.

An important question is how a virus with a segmented genome ensures that a full complement is present in the assembled virion. Many RNA viruses with segmented genomes can package them effectively to ensure all segments are accounted for to produce an infectious particle [2,91]. In Φ6 this is achieved by the controlled sequential packaging of the three segments [92], resulting in highly structured genome packing (Figure 7A,B). This is reminiscent of the packaging in dsDNA bacteriophages into a preformed head [93]. In contrast, the current model for the packaging of eukaryotic dsRNA viruses is a coalescence of the segments into a nucleoprotein particle that is then wrapped into a capsid shell in the reoviruses [2,91], or encased in a lipid envelope in the influenza virus [94]. In all cases, packaging signals in the form of RNA structural motifs direct the proper packaging process [92,95].

Many icosahedral virus capsids can self-assemble, often with the help of scaffolding partners [96,97]. In Φ6, the scaffolding role for P1 assembly is assumed mainly by P4, with assistance by P2 and P7 [16,57,58]. As with many procapsids, it assembles in a metastable state that can transform into a more stable mature form, in Φ6 concurrent with packaging and expansion (Figure 6).

The studies of the Φ6 procapsid and nucleocapsid structures grew with the development of better capabilities in electron microscopes as well as computational approaches to processing micrographs. The discovery of the locations of the P2 and P7 proteins was directly related to better reconstruction of cryoEM maps and examining difference maps between procapsids with different compositions [30,32,33]. Knowing these locations, we could count the presence of the molecules using cryo-electron tomography and obtain detailed distributions of occupancy [31]. New techniques to handle symmetry mismatch were developed for understanding the structures of P4, P2 and dsRNA within the context of the procapsid and nucleocapsid [45,46,67]. We combined X-ray crystallography of the P1 pentamer with the high resolution cryoEM maps of the procapsid and nucleocapsid to visualize the conformational differences between subunits and the transformations during capsid expansion [35]. We now have tools to study viruses in great structural detail, so that the success of a project is largely determined by the quality of sample preparation.

The remarkable progress in structural biology has given us a detailed understanding of the dsRNA and two inner layers of the Φ6 virion and its transformations during its life cycle. Nevertheless, there are many questions that remain to be answered. The full sequence of events in procapsid assembly would contribute to resolving how complete icosahedral particles form. How do the three ssRNA segments recognize the conformational state of the procapsid? How is the nucleocapsid enveloped in the final stages of virion formation? The detailed structures of the integral proteins in the envelope and the spike still needs to be determined. What triggers the lysis of the host cell? Structural details of the infection events are required to better understand how it binds to pili and breaches the cell envelope? After infection, is the P4 hexamer involved in the transmission of control from YajQ to the polymerase inside the P1 shell? There is ample room for further structural studies of the cystoviruses for their own sake but also in the broader context of protein interactions and dynamics, and not only pertinent to viruses.

Author Contributions: All aspects, JBH.

Funding: This project was funded using Federal funds from the Frederick National Laboratory for Cancer Research, National Institutes of Health (contract No. HHSN261200800001E).

Data Availability Statement: All structural data used in preparing the review can be found in the Electron Microscopy Databank (https://www.ebi.ac.uk/emdb) and the Protein Data Bank (https://www.rcsb.org).

Acknowledgments: In this section, you can acknowledge any support given which is not covered by the author contribution or funding sections. This may include administrative and technical support, or donations in kind (e.g., materials used for experiments).

Conflicts of Interest: The author declares no conflict of interest. The funders had no role in the design of the study; in the collection, analyses, or interpretation of data; in the writing of the manuscript; or in the decision to publish the results.

References

1. Vidaver, A.K.; Koski, R.K.; Van Etten, J.L. Bacteriophage phi6: a Lipid-Containing Virus of Pseudomonas phaseolicola. *J Virol* **1973**, *11*, 799-805, doi:10.1128/JVI.11.5.799-805.1973.
2. Borodavka, A.; Desselberger, U.; Patton, J.T. Genome packaging in multi-segmented dsRNA viruses: distinct mechanisms with similar outcomes. *Curr Opin Virol* **2018**, *33*, 106-112, doi:10.1016/j.coviro.2018.08.001.
3. Serrano-Aroca, A. Antiviral Characterization of Advanced Materials: Use of Bacteriophage Phi 6 as Surrogate of Enveloped Viruses Such as SARS-CoV-2. *Int J Mol Sci* **2022**, *23*, doi:10.3390/ijms23105335.
4. Chen, Y.G.; Hur, S. Cellular origins of dsRNA, their recognition and consequences. *Nat Rev Mol Cell Biol* **2022**, *23*, 286-301, doi:10.1038/s41580-021-00430-1.
5. Pinheiro, L.A.M.; Pereira, C.; Barreal, M.E.; Gallego, P.P.; Balcao, V.M.; Almeida, A. Use of phage varphi6 to inactivate Pseudomonas syringae pv. actinidiae in kiwifruit plants: in vitro and ex vivo experiments. *Appl Microbiol Biotechnol* **2020**, *104*, 1319-1330, doi:10.1007/s00253-019-10301-7.
6. Pinheiro, L.A.M.; Pereira, C.; Frazao, C.; Balcao, V.M.; Almeida, A. Efficiency of Phage phi6 for Biocontrol of Pseudomonas syringae pv. syringae: An in Vitro Preliminary Study. *Microorganisms* **2019**, *7*, doi:10.3390/microorganisms7090286.
7. de Carvalho, N.A.; Stachler, E.N.; Cimabue, N.; Bibby, K. Evaluation of Phi6 Persistence and Suitability as an Enveloped Virus Surrogate. *Environmental Science & Technology* **2017**, *51*, 8692-8700, doi:10.1021/acs.est.7b01296.
8. Frilander, M.; Poranen, M.; Bamford, D.H. The large genome segment of dsRNA bacteriophage phi6 is the key regulator in the in vitro minus and plus strand synthesis. *RNA* **1995**, *1*, 510-518.
9. Cuppels, D.A.; Van Etten, J.L.; Burbank, D.E.; Lane, L.C.; Vidaver, A.K. In vitro translation of the three bacteriophage phi 6 RNAs. *J. Virol.* **1980**, *35*, 249-251.
10. Bamford, D.H.; Romantschuk, M.; Somerharju, P.J. Membrane fusion in prokaryotes: bacteriophage phi 6 membrane fuses with the Pseudomonas syringae outer membrane. *EMBO J* **1987**, *6*, 1467-1473, doi:10.1002/j.1460-2075.1987.tb02388.x.
11. Mindich, L.; Lehman, J. Cell wall lysin as a component of the bacteriophage phi 6 virion. *J Virol* **1979**, *30*, 489-496.
12. Caldentey, J.; Bamford, D.H. The lytic enzyme of the Pseudomonas phage phi 6. Purification and biochemical characterization. *Biochim Biophys Acta* **1992**, *1159*, 44-50, doi:0167-4838(92)90073-M [pii].
13. Olkkonen, V.M.; Ojala, P.M.; Bamford, D.H. Generation of infectious nucleocapsids by in vitro assembly of the shell protein on to the polymerase complex of the dsRNA bacteriophage phi 6. *J Mol Biol* **1991**, *218*, 569-581.
14. Qiao, X.; Sun, Y.; Qiao, J.; Mindich, L. The role of host protein YajQ in the temporal control of transcription in bacteriophage Phi6. *Proc Natl Acad Sci U S A* **2008**, *105*, 15956-15960, doi:0807489105 [pii]10.1073/pnas.0807489105.
15. Mindich, L.; Davidoff-Abelson, R. The characterization of a 120 S particle formed during phi 6 infection. *Virology* **1980**, *103*, 386-391.
16. Gottlieb, P.; Strassman, J.; Bamford, D.H.; Mindich, L. Production of a polyhedral particle in Escherichia coli from a cDNA copy of the large genomic segment of bacteriophage phi 6. *J Virol* **1988**, *62*, 181-187.
17. Qiao, X.; Casini, G.; Qiao, J.; Mindich, L. In vitro packaging of individual genomic segments of bacteriophage phi 6 RNA: serial dependence relationships. *J Virol* **1995**, *69*, 2926-2931.
18. Johnson, M.D., 3rd; Mindich, L. Plasmid-directed assembly of the lipid-containing membrane of bacteriophage phi 6. *J Bacteriol* **1994**, *176*, 4124-4132.
19. Johnson, M.D., 3rd; Mindich, L. Isolation and characterization of nonsense mutations in gene 10 of bacteriophage phi 6. *J Virol* **1994**, *68*, 2331-2338.
20. Day, L.A.; Mindich, L. The molecular weight of bacteriophage phi 6 and its nucleocapsid. *Virology* **1980**, *103*, 376-385.
21. Mantynen, S.; Sundberg, L.R.; Poranen, M.M. Recognition of six additional cystoviruses: Pseudomonas virus phi6 is no longer the sole species of the family Cystoviridae. *Arch Virol* **2018**, *163*, 1117-1124, doi:10.1007/s00705-017-3679-4.
22. Makeyev, E.V.; Bamford, D.H. Replicase activity of purified recombinant protein P2 of double-stranded RNA bacteriophage phi6. *The EMBO journal* **2000**, *19*, 124-133, doi:10.1093/emboj/19.1.124.

23. Gottlieb, P.; Strassman, J.; Mindich, L. Protein P4 of the bacteriophage phi 6 procapsid has a nucleoside triphosphate-binding site with associated nucleoside triphosphate phosphohydrolase activity. *J Virol* **1992**, *66*, 6220-6222.
24. Paatero, A.O.; Syvaoja, J.E.; Bamford, D.H. Double-stranded RNA bacteriophage phi 6 protein P4 is an unspecific nucleoside triphosphatase activated by calcium ions. *J Virol* **1995**, *69*, 6729-6734.
25. Juuti, J.T.; Bamford, D.H. RNA binding, packaging and polymerase activities of the different incomplete polymerase complex particles of dsRNA bacteriophage phi 6. *J Mol Biol* **1995**, *249*, 545-554.
26. Juuti, J.T.; Bamford, D.H. Protein P7 of phage phi6 RNA polymerase complex, acquiring of RNA packaging activity by in vitro assembly of the purified protein onto deficient particles. *J Mol Biol* **1997**, *266*, 891-900.
27. Olkkonen, V.M.; Bamford, D.H. The nucleocapsid of the lipid-containing double-stranded RNA bacteriophage phi 6 contains a protein skeleton consisting of a single polypeptide species. *J Virol* **1987**, *61*, 2362-2367.
28. Butcher, S.J.; Dokland, T.; Ojala, P.M.; Bamford, D.H.; Fuller, S.D. Intermediates in the assembly pathway of the double-stranded RNA virus phi6. *Embo J* **1997**, *16*, 4477-4487.
29. Huiskonen, J.T.; de Haas, F.; Bubeck, D.; Bamford, D.H.; Fuller, S.D.; Butcher, S.J. Structure of the bacteriophage phi6 nucleocapsid suggests a mechanism for sequential RNA packaging. *Structure* **2006**, *14*, 1039-1048.
30. Sen, A.; Heymann, J.B.; Cheng, N.; Qiao, J.; Mindich, L.; Steven, A.C. Initial location of the RNA-dependent RNA polymerase in the bacteriophage Phi6 procapsid determined by cryo-electron microscopy. *J Biol Chem* **2008**, *283*, 12227-12231.
31. Nemecek, D.; Heymann, J.B.; Qiao, J.; Mindich, L.; Steven, A.C. Cryo-electron tomography of bacteriophage φ6 procapsids shows random occupancy of the binding sites for RNA polymerase and packaging NTPase. *J. Struct. Biol.* **2010**, *171*, 389-396, doi:10.1016/j.jsb.2010.06.005.
32. Katz, G.; Wei, H.; Alimova, A.; Katz, A.; Morgan, D.G.; Gottlieb, P. Protein P7 of the cystovirus phi6 is located at the three-fold axis of the unexpanded procapsid. *PloS one* **2012**, *7*, e47489, doi:10.1371/journal.pone.0047489.
33. Nemecek, D.; Qiao, J.; Mindich, L.; Steven, A.C.; Heymann, J.B. Packaging accessory protein P7 and polymerase P2 have mutually occluding binding sites inside the bacteriophage φ6 procapsid. *J. Virol.* **2012**, *86*, 11616-11624, doi:10.1128/JVI.01347-12.
34. Luque, D.; Mata, C.P.; Suzuki, N.; Ghabrial, S.A.; Caston, J.R. Capsid Structure of dsRNA Fungal Viruses. *Viruses* **2018**, *10*, doi:10.3390/v10090481.
35. Nemecek, D.; Boura, E.; Wu, W.; Cheng, N.; Plevka, P.; Qiao, J.; Mindich, L.; Heymann, J.B.; Hurley, J.H.; Steven, A.C. Subunit folds and maturation pathway of a dsRNA virus capsid. *Structure* **2013**, *21*, 1374-1383, doi:10.1016/j.str.2013.06.007.
36. Jaalinoja, H.T.; Huiskonen, J.T.; Butcher, S.J. Electron cryomicroscopy comparison of the architectures of the enveloped bacteriophages phi6 and phi8. *Structure* **2007**, *15*, 157-167.
37. Caspar, D.L.; Klug, A. Physical principles in the construction of regular viruses. *Cold Spring Harb Symp Quant Biol* **1962**, *27*, 1-24.
38. Juuti, J.T.; Bamford, D.H.; Tuma, R.; Thomas, G.J., Jr. Structure and NTPase activity of the RNA-translocating protein (P4) of bacteriophage phi 6. *J Mol Biol* **1998**, *279*, 347-359, doi:10.1006/jmbi.1998.1772.
39. El Omari, K.; Meier, C.; Kainov, D.; Sutton, G.; Grimes, J.M.; Poranen, M.M.; Bamford, D.H.; Tuma, R.; Stuart, D.I.; Mancini, E.J. Tracking in atomic detail the functional specializations in viral RecA helicases that occur during evolution. *Nucleic Acids Res* **2013**, *41*, 9396-9410, doi:10.1093/nar/gkt713.
40. de Haas, F.; Paatero, A.O.; Mindich, L.; Bamford, D.H.; Fuller, S.D. A symmetry mismatch at the site of RNA packaging in the polymerase complex of dsRNA bacteriophage phi6. *J Mol Biol* **1999**, *294*, 357-372.
41. Sun, X.; Bamford, D.H.; Poranen, M.M. Probing, by self-assembly, the number of potential binding sites for minor protein subunits in the procapsid of double-stranded RNA bacteriophage Phi6. *J. Virol.* **2012**, *86*, 12208-12216, doi:10.1128/JVI.01505-12.
42. Huiskonen, J.T.; Jaalinoja, H.T.; Briggs, J.A.; Fuller, S.D.; Butcher, S.J. Structure of a hexameric RNA packaging motor in a viral polymerase complex. *J Struct Biol* **2007**, *158*, 156-164.
43. Nemecek, D.; Cheng, N.; Qiao, J.; Mindich, L.; Steven, A.C.; Heymann, J.B. Stepwise expansion of the bacteriophage φ6 procapsid: possible packaging intermediates. *J. Mol. Biol.* **2011**, *414*, 260-271, doi:10.1016/j.jmb.2011.10.004.

44. Futerman, E. φ6 polymerase conformation; RNA packaging portal stability. City College of New York, CUNY, CUNY Academic Works, 2012.
45. Ilca, S.L.; Kotecha, A.; Sun, X.; Poranen, M.M.; Stuart, D.I.; Huiskonen, J.T. Localized reconstruction of subunits from electron cryomicroscopy images of macromolecular complexes. *Nat Commun* **2015**, *6*, 8843, doi:10.1038/ncomms9843.
46. Sun, Z.; El Omari, K.; Sun, X.; Ilca, S.L.; Kotecha, A.; Stuart, D.I.; Poranen, M.M.; Huiskonen, J.T. Double-stranded RNA virus outer shell assembly by bona fide domain-swapping. *Nat Commun* **2017**, *8*, 14814, doi:10.1038/ncomms14814.
47. Paatero, A.O.; Mindich, L.; Bamford, D.H. Mutational analysis of the role of nucleoside triphosphatase P4 in the assembly of the RNA polymerase complex of bacteriophage phi6. *J Virol* **1998**, *72*, 10058-10065.
48. Sinclair, J.F.; Mindich, L. RNA synthesis during infection with bacteriophage phi6. *Virology* **1976**, *75*, 209-217.
49. Gottlieb, P.; Strassman, J.; Qiao, X.Y.; Frucht, A.; Mindich, L. In vitro replication, packaging, and transcription of the segmented double-stranded RNA genome of bacteriophage phi 6: studies with procapsids assembled from plasmid-encoded proteins. *J Bacteriol* **1990**, *172*, 5774-5782.
50. Butcher, S.J.; Grimes, J.M.; Makeyev, E.V.; Bamford, D.H.; Stuart, D.I. A mechanism for initiating RNA-dependent RNA polymerization. *Nature* **2001**, *410*, 235-240.
51. Sarin, L.P.; Wright, S.; Chen, Q.; Degerth, L.H.; Stuart, D.I.; Grimes, J.M.; Bamford, D.H.; Poranen, M.M. The C-terminal priming domain is strongly associated with the main body of bacteriophage varphi6 RNA-dependent RNA polymerase. *Virology* **2012**, *432*, 184-193, doi:10.1016/j.virol.2012.05.035.
52. Poranen, M.M.; Koivunen, M.R.; Bamford, D.H. Nontemplated terminal nucleotidyltransferase activity of double-stranded RNA bacteriophage phi6 RNA-dependent RNA polymerase. *J Virol* **2008**, *82*, 9254-9264, doi:JVI.01044-08 [pii]10.1128/JVI.01044-08.
53. Poranen, M.M.; Salgado, P.S.; Koivunen, M.R.; Wright, S.; Bamford, D.H.; Stuart, D.I.; Grimes, J.M. Structural explanation for the role of Mn2+ in the activity of phi6 RNA-dependent RNA polymerase. *Nucleic Acids Res* **2008**, *36*, 6633-6644, doi:gkn632 [pii]10.1093/nar/gkn632.
54. Yang, H.; Makeyev, E.V.; Bamford, D.H. Comparison of polymerase subunits from double-stranded RNA bacteriophages. *J. Virol.* **2001**, *75*, 11088-11095, doi:10.1128/JVI.75.22.11088-11095.2001.
55. Wright, S.; Poranen, M.M.; Bamford, D.H.; Stuart, D.I.; Grimes, J.M. Noncatalytic ions direct the RNA-dependent RNA polymerase of bacterial double-stranded RNA virus varphi6 from de novo initiation to elongation. *J. Virol.* **2012**, *86*, 2837-2849, doi:10.1128/JVI.05168-11.
56. Qiao, J.; Mindich, L. The template specificity of bacteriophage Phi6 RNA polymerase. *J Virol* **2013**, *87*, 10190-10194, doi:10.1128/JVI.01467-13.
57. Sun, X.; Ilca, S.L.; Huiskonen, J.T.; Poranen, M.M. Dual Role of a Viral Polymerase in Viral Genome Replication and Particle Self-Assembly. *mBio* **2018**, *9*, doi:10.1128/mBio.01242-18.
58. Poranen, M.M.; Paatero, A.O.; Tuma, R.; Bamford, D.H. Self-assembly of a viral molecular machine from purified protein and RNA constituents. *Mol Cell* **2001**, *7*, 845-854, doi:S1097-2765(01)00228-3 [pii].
59. Eryilmaz, E.; Benach, J.; Su, M.; Seetharaman, J.; Dutta, K.; Wei, H.; Gottlieb, P.; Hunt, J.F.; Ghose, R. Structure and dynamics of the P7 protein from the bacteriophage phi 12. *J Mol Biol* **2008**, *382*, 402-422.
60. Wei, H.; Cheng, R.H.; Berriman, J.; Rice, W.J.; Stokes, D.L.; Katz, A.; Morgan, D.G.; Gottlieb, P. Three-dimensional structure of the enveloped bacteriophage phi12: an incomplete T = 13 lattice is superposed on an enclosed T = 1 shell. *PLoS One* **2009**, *4*, e6850, doi:10.1371/journal.pone.0006850.
61. Ikonen, T.; Kainov, D.; Timmins, P.; Serimaa, R.; Tuma, R. Locating the minor components of double-stranded RNA bacteriophage 6 by neutron scattering. *J. Appl. Crystall.* **2003**, *36*, 525-529, doi:doi:10.1107/S0021889803001857.
62. El Omari, K.; Sutton, G.; Ravantti, J.J.; Zhang, H.; Walter, T.S.; Grimes, J.M.; Bamford, D.H.; Stuart, D.I.; Mancini, E.J. Plate tectonics of virus shell assembly and reorganization in phage phi8, a distant relative of mammalian reoviruses. *Structure* **2013**, *21*, 1384-1395, doi:10.1016/j.str.2013.06.017.
63. Dokland, T. Scaffolding proteins and their role in viral assembly. *Cell Mol Life Sci* **1999**, *56*, 580-603, doi:10.1007/s000180050455.
64. Trask, S.D.; McDonald, S.M.; Patton, J.T. Structural insights into the coupling of virion assembly and rotavirus replication. *Nature reviews. Microbiology* **2012**, *10*, 165-177, doi:10.1038/nrmicro2673.

65. Frilander, M.; Bamford, D.H. In vitro packaging of the single-stranded RNA genomic precursors of the segmented double-stranded RNA bacteriophage phi 6: the three segments modulate each other's packaging efficiency. *J Mol Biol* **1995**, *246*, 418-428, doi:S0022283684700969 [pii].
66. Pirttimaa, M.J.; Paatero, A.O.; Frilander, M.J.; Bamford, D.H. Nonspecific nucleoside triphosphatase P4 of double-stranded RNA bacteriophage phi6 is required for single-stranded RNA packaging and transcription. *J Virol* **2002**, *76*, 10122-10127.
67. Ilca, S.L.; Sun, X.; El Omari, K.; Kotecha, A.; de Haas, F.; DiMaio, F.; Grimes, J.M.; Stuart, D.I.; Poranen, M.M.; Huiskonen, J.T. Multiple liquid crystalline geometries of highly compacted nucleic acid in a dsRNA virus. *Nature* **2019**, *570*, 252-256, doi:10.1038/s41586-019-1229-9.
68. Liu, H.; Cheng, L. Cryo-EM shows the polymerase structures and a nonspooled genome within a dsRNA virus. *Science* **2015**, *349*, 1347-1350, doi:10.1126/science.aaa4938.
69. Zhang, X.; Ding, K.; Yu, X.; Chang, W.; Sun, J.; Zhou, Z.H. In situ structures of the segmented genome and RNA polymerase complex inside a dsRNA virus. *Nature* **2015**, *527*, 531-534, doi:10.1038/nature15767.
70. Strauss, S.; Acker, J.; Papa, G.; Desiro, D.; Schueder, F.; Borodavka, A.; Jungmann, R. Principles of RNA recruitment to viral ribonucleoprotein condensates in a segmented dsRNA virus. *Elife* **2023**, *12*, doi:10.7554/eLife.68670.
71. Tuma, R.; Bamford, J.K.; Bamford, D.H.; Thomas, G.J., Jr. Assembly dynamics of the nucleocapsid shell subunit (P8) of bacteriophage phi6. *Biochemistry* **1999**, *38*, 15025-15033, doi:10.1021/bi991473p.
72. Cvirkaite-Krupovic, V.; Poranen, M.M.; Bamford, D.H. Phospholipids act as secondary receptor during the entry of the enveloped, double-stranded RNA bacteriophage phi6. *J Gen Virol* **2010**, *91*, 2116-2120, doi:vir.0.020305-0 [pii]10.1099/vir.0.020305-0.
73. Romantschuk, M.; Olkkonen, V.M.; Bamford, D.H. The nucleocapsid of bacteriophage phi 6 penetrates the host cytoplasmic membrane. *Embo J* **1988**, *7*, 1821-1829.
74. Laurinavicius, S.; Kakela, R.; Bamford, D.H.; Somerharju, P. The origin of phospholipids of the enveloped bacteriophage phi6. *Virology* **2004**, *326*, 182-190, doi:10.1016/j.virol.2004.05.021S004268220400371X [pii].
75. Sinclair, J.F.; Tzagoloff, A.; Levine, D.; Mindich, L. Proteins of bacteriophage phi6. *J Virol* **1975**, *16*, 685-695.
76. Van Etten, J.; Lane, L.; Gonzalez, C.; Partridge, J.; Vidaver, A. Comparative properties of bacteriophage phi6 and phi6 nucleocapsid. *J Virol* **1976**, *18*, 652-658.
77. Stitt, B.L.; Mindich, L. The structure of bacteriophage phi 6: protease digestion of phi 6 virions. *Virology* **1983**, *127*, 459-462.
78. Stitt, B.L.; Mindich, L. Morphogenesis of bacteriophage phi 6: a presumptive viral membrane precursor. *Virology* **1983**, *127*, 446-458.
79. Lyytinen, O.L.; Starkova, D.; Poranen, M.M. Microbial production of lipid-protein vesicles using enveloped bacteriophage phi6. *Microb Cell Fact* **2019**, *18*, 29, doi:10.1186/s12934-019-1079-z.
80. Kenney, J.M.; Hantula, J.; Fuller, S.D.; Mindich, L.; Ojala, P.M.; Bamford, D.H. Bacteriophage phi 6 envelope elucidated by chemical cross-linking, immunodetection, and cryoelectron microscopy. *Virology* **1992**, *190*, 635-644.
81. Leo-Macias, A.; Katz, G.; Wei, H.; Alimova, A.; Katz, A.; Rice, W.J.; Diaz-Avalos, R.; Hu, G.B.; Stokes, D.L.; Gottlieb, P. Toroidal surface complexes of bacteriophage varphi12 are responsible for host-cell attachment. *Virology* **2011**, *414*, 103-109, doi:10.1016/j.virol.2011.03.020.
82. Emori, Y.; Iba, H.; Okada, Y. Semi-conservative transcription of double-stranded RNA catalyzed by bacteriophage phi 6 RNA polymerase. *J Biochem* **1980**, *88*, 1569-1575.
83. Coplin, D.L.; Van Etten, J.L.; Koski, R.K.; Vidaver, A.K. Intermediates in the biosynthesis of double-stranded ribonucleic acids of bacteriophage phi 6. *Proc Natl Acad Sci U S A* **1975**, *72*, 849-853.
84. Emori, Y.; Iba, H.; Okada, Y. Transcriptional regulation of three double-stranded RNA segments of bacteriophage phi 6 in vitro. *J Virol* **1983**, *46*, 196-203.
85. Ojala, P.M.; Bamford, D.H. In vitro transcription of the double-stranded RNA bacteriophage phi 6 is influenced by purine NTPs and calcium. *Virology* **1995**, *207*, 400-408, doi:10.1006/viro.1995.1099.
86. Miron, S.; Borza, T.; Saveanu, C.; Gilles, A.M.; Barzu, O.; Craescu, C.T. 1H, 13C and 15N resonance assignment of YajQ, a protein of unknown structure and function from Escherichia coli. *J Biomol NMR* **2001**, *20*, 287-288.
87. Qiao, J.; Qiao, X.; Sun, Y.; Mindich, L. Role of host protein glutaredoxin 3 in the control of transcription during bacteriophage Phi2954 infection. *Proc Natl Acad Sci U S A* **2010**, *107*, 6000-6004, doi:1000383107 [pii]10.1073/pnas.1000383107.

88. Qiao, X.; Sun, Y.; Qiao, J.; Mindich, L. Interaction of a host protein with core complexes of bacteriophage phi6 to control transcription. *J Virol* **2010**, *84*, 4821-4825, doi:JVI.00026-10 [pii]10.1128/JVI.00026-10.
89. Heymann, J.B.; Nemecek, D.; Huang, R.; Cheng, N.; Qiao, J.; Mindich, L.; Steven, A.C. A Polymerase-Activating Host Factor, YajQ, Bound to the Bacteriophage ϕ6 Capsid. *Microscopy and Microanalysis* **2016**, *22*, 1110-1111, doi:10.1017/S1431927616006395.
90. Teplyakov, A.; Obmolova, G.; Bir, N.; Reddy, P.; Howard, A.J.; Gilliland, G.L. Crystal structure of the YajQ protein from Haemophilus influenzae reveals a tandem of RNP-like domains. *J Struct Funct Genomics* **2003**, *4*, 1-9.
91. McDonald, S.M.; Nelson, M.I.; Turner, P.E.; Patton, J.T. Reassortment in segmented RNA viruses: mechanisms and outcomes. *Nat Rev Microbiol* **2016**, *14*, 448-460, doi:10.1038/nrmicro.2016.46.
92. Mindich, L. Precise packaging of the three genomic segments of the double-stranded-RNA bacteriophage phi6. *Microbiol Mol Biol Rev* **1999**, *63*, 149-160.
93. Rao, V.B.; Feiss, M. Mechanisms of DNA Packaging by Large Double-Stranded DNA Viruses. *Annu Rev Virol* **2015**, *2*, 351-378, doi:10.1146/annurev-virology-100114-055212.
94. Haralampiev, I.; Prisner, S.; Nitzan, M.; Schade, M.; Jolmes, F.; Schreiber, M.; Loidolt-Kruger, M.; Jongen, K.; Chamiolo, J.; Nilson, N.; et al. Selective flexible packaging pathways of the segmented genome of influenza A virus. *Nat Commun* **2020**, *11*, 4355, doi:10.1038/s41467-020-18108-1.
95. Ye, L.; Ambi, U.B.; Olguin-Nava, M.; Gribling-Burrer, A.S.; Ahmad, S.; Bohn, P.; Weber, M.M.; Smyth, R.P. RNA Structures and Their Role in Selective Genome Packaging. *Viruses* **2021**, *13*, doi:10.3390/v13091788.
96. Selivanovitch, E.; Douglas, T. Virus capsid assembly across different length scales inspire the development of virus-based biomaterials. *Curr Opin Virol* **2019**, *36*, 38-46, doi:10.1016/j.coviro.2019.02.010.
97. Perlmutter, J.D.; Hagan, M.F. Mechanisms of virus assembly. *Annu Rev Phys Chem* 2015, *66*, 217-239, doi:10.1146/annurev-physchem-040214-121637.